HHS Public Access

Author manuscript

J Control Release. Author manuscript; available in PMC 2021 November 18.

Published in final edited form as:

J Control Release. 2021 November 10; 339: 553–561. doi:10.1016/j.jconrel.2021.08.040.

Genetic *in situ* engineering of myeloid regulatory cells controls inflammation in autoimmunity

N.N. Parayath[a], **S. Hao**[a], **S.B. Stephan**[a], **A.L. Koehne**[b], **C.E. Watson**[b], **M.T. Stephan**[a,c,*]

[a]Clinical Research Division, Fred Hutchinson Cancer Research Center, Seattle, WA 98109, USA

[b]Translational Pathology, Fred Hutchinson Cancer Research Center, Seattle, WA 98109, USA

[c]Department of Bioengineering and Molecular Engineering & Sciences Institute, University of Washington, Seattle 98195, WA, USA

Abstract

The ability of myeloid regulatory cells (MRCs) to control immune responses and to promote tolerance has prompted enormous interest in exploiting them therapeutically to treat inflammation, autoimmunity, or to improve outcomes in transplantation. While immunomodulatory small-molecule compounds and antibodies have provided relief for some patients, the dosing entails high systemic drug exposures and thus increased risk of off-target adverse effects. More recently, MRC-based cell-therapy products have entered clinical testing for tolerance induction. However, the elaborate and expensive protocols currently required to manufacture engineered MRCs *ex vivo* put this approach beyond the reach of many patients who might benefit. A solution could be to directly program MRCs *in vivo*. Here we describe a targeted nanocarrier that delivers *in vitro*-transcribed mRNA encoding a key anti-inflammatory mediator. We demonstrate in models of systemic lupus erythematosus that infusions of nanoparticles formulated with mRNA encoding glucocorticoid-induced leucine zipper (GILZ) effectively control the disease. We further establish that these nanoreagents are safe for repeated dosing. Implemented in the clinic, this new therapy could enable physicians to treat autoimmune disease while avoiding systemic treatments that disrupt immune homeostasis.

Keywords

In situ gene therapy; mRNA; Autoimmune disease; Glucocorticoid-induced leucine zipper

*Corresponding author at: Clinical Research Division, Fred Hutchinson Cancer Research Center, Seattle, WA 98109, USA. mstephan@fredhutch.org (M.T. Stephan).

Credit author statement

N.N.P. and S.H. designed and performed experiments and analyzed and interpreted data, S.B.S. manufactured nanoparticles, A.L.K. and C.E.W. performed the histopathological analysis, and M.T.S designed the study, performed experiments, analyzed and interpreted data, and wrote the manuscript.

Declaration of Competing Interest

M.T.S. is a consultant and scientific founder of Tidal Therapeutics (a Sanofi company). The remaining authors declare no competing interest.

Appendix A. Supplementary data

Supplementary data to this article can be found online at https://doi.org/10.1016/j.jconrel.2021.08.040.

1. Introduction

Myeloid cells play an essential role in maintaining the balance between inflammation and tolerance [1,2]. Over the years, researchers have gained a basic understanding of the principles that underlie myeloid cell activation during infection and in acute inflammation, and how resolution of this normal physiological response goes wrong in autoimmune disease or transplant rejection. In particular, myeloid regulatory cells (MRCs), which include polymorphonuclear neutrophils, macrophages, myeloid-derived suppressor cells, and dendritic cells, have emerged as therapeutic targets, based on their potential to counter-regulate inflammation, maintain tissue homeostasis, and promote tolerance [3,4]. Traditionally, non-steroidal anti-inflammatory drugs (NSAIDs) and glucocorticoids are used in the treatment of autoimmune inflammatory diseases. Although generally effective, NSAIDs have adverse effects, such as ulcers, kidney injury, and bleeding in the gastrointestinal tract [5]. Similarly, glucocorticoid use carries a significant burden of toxicity, including higher risks of opportunistic infections, iatrogenic osteoporosis and avascular necrosis, cardiovascular events, cataracts and glaucoma, as well as psychiatric adverse effects like psychosis and manic episodes [6]. In the past two decades, biologies targeting tumor necrosis factor (TNF) have been developed [7,8]. TNF is generally considered to be the master pro-inflammatory cytokine and plays a crucial role in the pathogenesis of inflammatory diseases. Consequently, anti-TNF therapy has become a mainstay treatment for autoimmune diseases. Nevertheless, up to 40% of patients have no response to anti-TNF drugs [9]. Furthermore, this treatment is associated with adverse effects such as increased risk of infection, and has even triggered the *de novo* development of autoimmune diseases [10]. These harmful effects of anti-TNF treatment are likely caused by systemic inhibition of TNF biological functions.

To avoid exposing patients to high systemic doses of immunosuppressive agents, investigators began exploring MRCs as cell-therapy products that can be (i) generated *ex vivo*, (ii) expanded to clinically relevant numbers, and (iii) reinfused to swiftly re-establish tolerance in autoimmune disease or after transplantation [11]. In particular, tolerogenic dendritic cells and regulatory macrophages have proven beneficial as a cell-based immunosuppressive therapy, and clinical-grade protocols for manufacturing these cell types have been optimized [12,13]. However, the complexity and high costs involved in manufacturing a bespoke cell product for each patient, as opposed to preparing a drug in bulk in a standardized form, make it difficult to compete with *frontline therapy* options such as small-molecule drugs or monoclonal antibodies. The entire process has to be conducted under environmentally controlled good manufacturing practices (GMP)-compliant conditions, which are expensive to maintain and run. Because each MRC product is made from starting materials (peripheral blood) from the patient to be treated, there are no economies of scale.

In vitro-transcribed (IVT) mRNA has recently come into focus as a potential new drug class to deliver genetic information into cells [14,15]. Such synthetic mRNA medicines structurally resemble natural mRNA and can be engineered to transiently express proteins. They are easily developed, inexpensive, and efficiently *scalable* for manufacturing purposes. Advances in addressing the inherent challenges of this drug class, particularly related

to controlling the translational efficacy and immunogenicity of the IVT mRNA [16-19], provide the basis for a broad range of potential applications.

Here, we explore the use of IVT mRNA as an injectable drug to genetically program circulating myeloid cells with potent immunosuppressive functions (Fig. 1). To condense and protect the IVT mRNA payload and to target disease-causing inflammatory myeloid cells, we formulated biodegradable polymeric nanocarriers. For cell-specific targeting, we functionalized nanoparticles with an antibody fragment against CD64, whose expression is strongly elevated on monocytes, macrophages, dendritic cells and neutrophils in patients with inflammatory autoimmune disease [20].

To supply the targets with a gene encoding a master regulator of anti-inflammatory and immunosuppressive effects, we loaded the particles with mRNA encoding glucocorticoid-induced leucine zipper (GILZ) protein. First identified in 1997 by subtractive hybridization after its dramatic induction by dexamethasone in murine lymphoid tissue [21], GILZ was subsequently found to be a pivotal endogenous regulator of inflammation and the immune response [22]. Importantly, in autoimmune disease, such as systemic lupus erythematosus (SLE), rheumatoid arthritis, inflammatory bowel disease, ankylosing spondylitis, psoriasis, and asthma, GILZ is under-expressed and correlates negatively with disease activity [23-26].

Using an *in vivo* mouse test system that faithfully models SLE [27], we establish that serial intravenous administration of GILZ-encoding nanoparticles effectively alleviates manifestations of lupus pathogenesis and lengthens life span. Moreover, we show that this therapy triggers a broad spectrum of actions on various immune cells, beyond reprogramming the myeloid compartment, including B cells, T cells and natural killer (NK) cells, all of which are known to drive the inflammatory response in SLE. This sweeping immunomodulatory effect substantially reduces the levels of pro-inflammatory cytokines and autoantibodies and ameliorates tissue damage and organ failure. Based on these data, future work will entail developing a robust protocol for the scaled-up production of CD64-targeted GILZ-mRNA nanoparticles under GMP-conditions so they can be carried forward into large primate and human studies.

2. Materials and methods

2.1. Human samples

Human SLE patient whole blood samples were obtained from Humancells Biosciences (Fremont, CA).

2.2. Cell lines

RAW246.7 cells were purchased from ATCC and cultured in DMEM supplemented 10% fetal bovine serum (FBS). THP1-Lucia™ NF-κB cells (NF-κB-inducible reporter monocytes) were purchased from InvivoGen (Cat# thp1-nfkb) and cultured in RPMI 1640, 2 mM L-glutamine, 25 mM HEPES, 10% heat-inactivated FBS, 100 μg/ml Normocin™, Pen-Strep (100 U/ml-100 μg/ml).

2.3. mRNA

Codon-optimized mRNAs for eGFP and GILZ were obtained from TriLink Biotechnologies. mRNA transcript was modified with full substitution of N1-Methyl-Pseudo-U Capped using CleanCap® AG poly-adenylated (120A), DNase and phosphatase treatment and purified by silica membrane followed by HPLC purification.

2.4. PbAE synthesis

1,4-Butanediol diacrylate was combined with 4-amino-1-butanol in a 1:1 M ratio of diacrylate to amine monomers. Acrylate-terminated poly (4-amino-1-butanol-*co*-1,4-butanediol diacrylate) was formed by heating the mixture to 90°C with stirring for 24h. 2.3g of this polymer was dissolved in 2 ml tetrahydrofuran (THF). To form the piperazine-capped 447 polymer, 786mg of 1-(3-aminopropyl) — 4-methylpiperazine in 13 ml THF was added to the polymer/THF solution and stirred at room temperature (RT) for 2 h. The capped polymer was precipitated with 5 volumes of diethyl ether, washed with 2 volumes of fresh ether, and dried under vacuum for 1 day. Neat polymer was dissolved in dimethyl sulfoxide (DMSO) to a concentration of 100 mg/ml and stored at −20°C.

2.5. Antibody digestion to F(ab) fragment

Purified anti-mouse CD64 (FcγRI) antibody (clone: X54-5/7.1) and Purified Mouse IgG1, κ Isotype Ctrl Antibody were obtained from Bio-legend and digested using a Pierce™ Mouse IgG1 Fab and F(ab')2 Preparation Kit (ThermoFisher Scientific) as per the manufacturer's instructions. Purified F(ab) fragments were conjugated to PGA within 24 h of digestion.

2.6. PGA conjugation to F(ab) fragment

Poly(L-glutamic acid sodium salt) MW = 15,000 Da, Alamanda Polymers) was dissolved in water to 20 mg/ml then sonicated for 10 min in a bath sonicator. An equal volume of EDC•HCl (Thermo Fisher Scientific in water (4 mg/ml, 16 equiv.) was added and the solution was mixed at RT for 5 min. The activated PGA was added to a solution of F(ab) protein in PBS at a 4:1 M ratio. The solution was mixed at RT for 4 h. Excess reagents were removed by diafiltration with PBS (Amicon Ultra centrifugal filter, 30 kDa MWCO). Protein concentration was determined using a NanoDrop 2000 Spectrophotometer (Thermo Scientific, Waltham, MA).

2.7. Nanoparticle preparation

GILZ mRNA or GFP mRNA was diluted to 100 μg/mL in 25 mM sodium acetate (NaOAc) buffer (pH = 5.2). PbAE-447 polymer in DMSO (prepared as described previously [28]) was diluted from 100 μg/μl to 6 μg/μl in NaOAc buffer. To form the nanoparticles, PbAE-447 polymers were added to the mRNA at a ratio of 60:1 (w:w) and vortexed immediately for 15 s at medium speed, then the mixture was incubated at RT for 5 min to allow the formation of PbAE-mRNA polyplexes. In the next step, 0.5 μg/μl PGA-CD64 F(ab) in NaOAc buffer was added to the polyplexes solution, vortexed for 15 s at medium speed, and incubated for 5 min at RT. In this process, PGA-CD64 F(ab) coated the surfaces of PbAE-mRNA polyplexes to form the final nanoparticles. For long-term storage, D-sucrose (60 mg/mL) was added to the nanoparticle solutions as a cryoprotectant. The nanoparticles were snap-frozen in dry ice,

then lyophilized. The dried nanoparticles were stored at −20 °C or −80 °C until use. For *in vivo* experiments, lyophilized nanoparticles were resuspended in water at a 1:20 (w:v) ratio.

2.8. Characterization of nanoparticle size distribution and ζ-potential

The physiochemical properties of nanoparticles (including hydrodynamic radius, polydispersity, ζ-potential, and stability) were characterized using a Zetapals instrument (Brookhaven Instrument Corporation) at 25 °C. To measure the hydrodynamic radius and polydispersity based on dynamic light scattering, nanoparticles were diluted fivefold into 25 mM NaOAc (pH = 5.2). To measure the ζ-potential, nanoparticles were diluted 10-fold in 10 mM PBS (pH = 7.0). To assess the stability of nanoparticles, freshly prepared particles were diluted in 10 mM PBS buffer (pH = 7.4). The hydrodynamic radius and polydispersity of nanoparticles were measured every 10 min for 5 h, and their sizes and particle concentrations were derived from Particle Tracking Analysis using a Nanosite 300 instrument (Malvern).

2.9. CD64 F(ab) targeting efficiency in RAW 246 cells

RAW 246 cells were seeded on 6-well plates in conditioned medium (LPS, 20 ng/ml and INFγ, 20 ng/ml) for 24 h before transfection, which induced cellular pro-inflammatory phenotypes. RAW 246 macrophages were then treated with 2.5 μg GFP mRNA nanoparticles with either PGA conjugated to CD64 antibody Fab fragment or unconjugated PGA. After 6 h, the cells were washed and incubated in conditioned medium for another 24 h before flow cytometry analysis for GFP expression.

2.10. mRNA transfection kinetics in RAW 246 cells

RAW 246 cells were seeded on 6-well plates in conditioned medium (LPS, 20 ng/ml and INFγ, 20 ng/ml) for 24 h before transfection, which induced cellular pro-inflammatory phenotypes. RAW 246 macrophages were then treated with GILZ nanoparticles containing 2.5 μg mRNA. After 6 h, the cells were washed and incubated in conditioned medium for 6, 12, 24, 48, 72, and 96 h before RNA isolation. RNAs were extracted from these cells for qRT-PCR analysis and compared to RNA extracted from untreated RAW 246 cells grown in conditioned medium.

2.11. Flow cytometry and cell sorting

Human cells obtained from synovial fluid of rheumatoid arthritis patients and blood samples of SLE patients were analyzed by flow cytometry using the anti-human antibody probes listed in Supplementary Table 1. Mouse cells obtained from blood, spleen, kidney, and lymph nodes were analyzed by flow cytometry with myeloid and lymphoid immunophenotyping panels using the anti-mouse antibody probes listed in Supplementary Tables 2 and 3. Data were collected using a BD LSRFortessa analyzer running FACSDIVA software (Beckton Dickinson). CD11b + monocytes were sorted using BD FACS ARIA II. All collected data were analyzed using FlowJo 10.0 software.

2.12. Cytokine analysis

Cytokine levels were evaluated using a Luminex 200 system (Luminex) at the FHCRC Immune Monitoring shared resource. Mouse plasma concentrations of INFγ and IL-6 were measured.

2.13. Anti-dsDNA antibody (IgG) ELISA

Mouse plasma concentration of anti-dsDNA antibody (IgG) was measured using a Mouse anti-dsDNA IgG-specific ELISA Kit (Alpha Diagnostics International, Inc).

2.14. Urea nitrogen (BUN) levels

Mouse urea nitrogen (BUN) levels were measured calorimetrically using a Urea Nitrogen (BUN) Colorimetric Detection Kit (Fisher Scientific).

2.15. qRT-PCR analysis

Gene expression levels were determined by qRT-PCR. To measure codon-optimized GILZ, endogenous GILZ, and housekeeping ACTB genes, total RNA was isolated with RNeasy mini-columns (Qiagen) according to the manufacturer's instructions. cDNA was synthesized using a High-Capacity RNA-to-cDNA™ Kit (Applied Biosystems). For each sample, qRT-PCR was performed in triplicate with PerfeCTa qPCR SuperMix Low ROX (Quanta) using gene-specific probes from Roche's Universal Probe Library (UPL) and PCR primers optimized by Probe-Finder (Roche): codon-optimized GILZ, UPL-050, F- CAATCCTGTTGTTCTTCCACTCT, R- TCCATTGCCTGCTCAATTTT; endogenous GILZ, UPL-68, F- CCCTAGACAACAAGATTGAGCA, R- TCTTCTCAAGCAGCTCACGA. mRNA levels were normalized based on amplification of the Universal Probe Library Mouse ACTB Gene Assay (#05046190001). All qRT-PCRs were performed using Quant Studio5 RT-PCR machines running QuantStudio6 software (Applied Biosystems). In cases when the amplification plot did not cross the threshold and no Ct value was obtained ("undetermined"), a Ct value equal to the highest cycle number in the assay (40 cycles) was used for comparisons of relative expression.

2.16. Inflammatory monocyte signature gene analysis using NanoString technology

Gene expression values from CD11b + sorted cells from mouse blood samples were measured using the nCounter® Myeloid Innate Immunity Panel (NanoString Technology), which analyzes 770 genes occurring in 19 different pathways and processes them across seven different myeloid cell types. The samples were tested using an nCounter Analysis System (NanoString Technologies). Raw data were processed and checked for quality using the R/Bioconductor NanoStringQCPro software package. Expression values were normalized to the geometric mean of housekeeping genes and log2-transformed using nSolver 4.0 software (NanoString Technologies). False Discovery Rates for ratio data were calculated from the *p*-values returned by the *t*-tests using the Benjamini-Yekutieli method.

2.17. NFkB inhibition assay

THP1-LuciaTM NF-κB cells were seeded in 24-well plates with *phorbol 12-myristate 13-acetate* (PMA; 100 ng/ml) for 24 h to induce differentiation of macrophages. After 24 h,

adhered cells were washed, and cells were incubated in fresh medium (without PMA) for 72 h. After 72 h, the cells were incubated in conditioned medium (LPS, 20 ng/ml and INFγ, 20 ng/ml) for 72 h before transfection. The cells were then treated with GFP nanoparticles (1.5 μg mRNA) or GILZ nanoparticles (1.5 or 1 or 0.75 μg mRNA) for 6 h. After 6 h, the cells were washed and incubated in conditioned medium for 24 h before IVIS imaging.

2.18. SLE mouse model

All mice used in these experiments were obtained from Jackson Laboratory (Strain- MRL/MpJ-*Fas*^{lpr}/J, Stock No: 000485). All of the mice were used in the context of a protocol approved by the center's Institutional Animal Care and Use Committee. Female MRL/MpJ-*Fas*^{lpr}/J mice were obtained at 8 weeks of age.

2.19. Biodistribution studies

For the GFP mRNA-based biodistribution studies, once the mice reached 12 weeks of age, they were divided in two groups (6 mice/group). Mice were intravenously administered PBAE nanoparticles containing 25 μg GFP mRNA with PGA conjugated to either CD64 antibody Fab fragment (group 1) or isotype antibody Fab fragment (group 2) on days 1 and 2, followed by two doses on day 3. All the mice were euthanized with CO2 at 24 h following the last dose. Whole blood and spleens were collected from both groups for flow cytometric analysis.

2.20. Efficacy and mechanism studies

Mice 11 weeks of age were divided into four groups (10 mice/group). Group 1 received intravenously administered PBAE nanoparticles containing 25 μg GILZ mRNA with PGA conjugated to CD64 antibody Fab fragment per dose, with 3 doses given per week for 6 weeks. Group 2 received intravenously administered PBAE nanoparticles containing 25 μg GFP mRNA with PGA conjugated to CD64 antibody Fab fragment per dose, with 3 doses given per week for 6 weeks. Group 3 received intravenously administered dexamethasone (Selleck Chemicals LLC) (4 mg/kg/week) for 6 weeks. Group 4 received intravenously administered PBS (equal to the volume given to the nanoparticle-treated groups) for 6 weeks. Blood (~150 μl) was collected retro-orbitally from all the mice once a week from 14 to 20 weeks of age. Once mice reached 20 weeks of age, they were euthanized with CO2 and whole blood all the organs were retrieved. Blood was collected for serum chemistry, cytokine profile analyses (performed by Phoenix Central Laboratories, Mukilteo, WA), dsDNA antibody ELISA and flow cytometric analysis. All the organs were divided into halves, and one half was fixed in 4% paraformaldehyde for further sectioning and staining with H&E. The specimens were interpreted by board-certified staff pathologists, in a blinded fashion. The other halves of the organs (spleen, kidney, lymph nodes) were retrieved for flow cytometric analysis.

2.21. In vivo bioluminescence imaging

A XenoLight RediJect Inflammation probe (PerkinElmer, #760536) was used for monitoring inflammation (myeloperoxidase activity of activated phagocytes) throughout the efficacy study duration. Mice were anesthetized with 2% isoflurane (Forane, Baxter Healthcare)

before and during imaging. Each mouse was injected intraperitoneally with 200 μL of Xenolight in PBS (40 mg/mL), and images were collected 10 min later. Bioluminescence images were collected with a Xenogen IVIS Spectrum Imaging System (Xenogen) and acquisition time of 5 min.

2.22. Survival studies

Mice 11 weeks of age were divided into four groups (10 mice/group). Group 1 received intravenously administered PBAE nanoparticles containing 25 μg GILZ mRNA with PGA conjugated to CD64 antibody Fab fragment per dose, with 3 doses given per week for 6 weeks. Group 2 received intravenously administered PBAE nanoparticles containing 25 μg GFP mRNA with PGA conjugated to CD64 antibody Fab fragment per dose, with 3 doses given per week for 6 weeks. Group 3 received intravenously administered dexamethasone (Selleck Chemicals LLC) (4 mg/kg/week) for 6 weeks. Group 4 received intravenously administered PBS (equal to the volume given to the nanoparticle-treated groups) for 6 weeks. Mice were monitored weekly and euthanized when their health declined, according to care guidelines.

2.23. Statistical analysis

The statistical significance of observed differences was analyzed using the unpaired, two-tailed Student's *t*-test or the unpaired, two-tailed one-way ANOVA test. The *P* values for each measurement are listed in the figures or figure legends. We characterized survival data using the Log-rank test. All statistical analyses were performed using GraphPad Prism software version 6.0.

2.24. Study approval

The care and use of mice in this study were approved by the Institutional Animal Care & Use Committee (IACUC) at the Fred Hutchinson Cancer Research Center, and complied with all relevant ethical regulations for animal testing and research (Assurance #A3226–01, IACUC Protocol Number 50782).

3. Results

3.1. CD64-targeted mRNA nanocarriers efficiently transfect inflammatory myeloid cells

Several studies on patient samples have documented upregulated levels of the high-affinity receptor for IgG FcγRI/CD64 on activated monocytes, dendritic cells, macrophages, mast cells, and neutrophils at sites of chronic inflammation [20]. As a first step, we confirmed by flow cytometry that peripheral blood mononuclear cells isolated from SLE patients are activated and exhibit increased surface expression of CD64 (Fig. 2a). To faithfully recapitulate this clinical scenario in an immunocompetent mouse model, we used MRL/MpJ-Fas^{lpr}/J (MRL-lpr) *mice*, which develop rapid and severe lupus-like disease [27]. Untreated, these mice die at an average age of 24 weeks from systemic autoimmunity, massive lymphadenopathy associated with proliferation of aberrant T cells, arthritis, and immune complex glomerulonephrosis. As in human SLE, peripheral blood cells isolated from MRL-lpr mice express CD64, especially in monocytes and NK cells, but also macrophages and circulating dendritic cells (Fig. 2b).

To deliver mRNA encoding the anti-inflammatory GILZ protein to CD64+ cells, we used a biodegradable poly(β-amino ester) (PBAE) polymer formulation as a carrier matrix. Cationic PBAE self-assembles into nanocomplexes with anionic nucleic acids *via* electrostatic interactions. The particles were made cell-targeting by coupling an anti-CD64 antigen binding fragment (Fab) to polyglutamic acid (PGA; Fig. 2c), forming a conjugate that was electrostatically adsorbed to the particles. The resulting mRNA nanocarriers can be lyophilized for long-term storage (Fig. 2d). We used Particle Tracking Analysis (NanoSight NS300, Malvern Panalytical) to characterize the particles manufactured in 5 independent batches (Fig. 2e). The PbAE/PGA-anti-CD64 nanoparticles had a mean diameter of 104 nm ± 36.2 nm, a ζ potential of −14.45 mV ± 6.4 mV, and the mRNA encapsulation was 91.4 ± 6.3%.

To examine the extent to which the nanoparticle interactions were confined to inflammatory cells, we intravenously infused MRL/lpr mice with anti-CD64 Fab- (or isotype control-) functionalized particles formulated with green fluorescent protein-encoding mRNA (GFP-NPs; Fig. 2f). Transfection rates in peripheral blood cells were analyzed by flow cytometry measurements of GFP expression. We found that surface-modification of the particles with anti-CD64 Fabs was relevant, as the transfection rates for isotype control-functionalized nanocarriers dropped, particularly in macrophages and dendritic cells (4.4-fold and 2.9-fold, respectively; Fig. 2g). In other inherently phagocytic cell types, such as circulating monocytes, high transfection rates were achieved independent of nanoparticle targeting.

3.2. In vivo biological activity of anti-CD64 GILZ mRNA nanoparticles

To evaluate the therapeutic potential of CD64-targeted GILZ-encoding mRNA nanoparticles, we treated MRL/lpr mice starting at 10 weeks of age. By this stage, mice begin developing the hallmark serological markers and peripheral pathologies typifying lupus. The animals were divided into 3 groups that received either PBS (control), GFP mRNA nanoparticles (sham), or GILZ mRNA nanoparticles at an intravenous dose of 75 μg mRNA/mouse/week for 6 weeks (Fig. 3a). Every two weeks, serum titers of anti-double-stranded DNA (dsDNA) autoantibody and pro-inflammatory cytokines were quantified by ELISA. Half of the animals were euthanized at week 20 and a complete gross and microscopic necropsy was performed by a board-certified staff pathologist. The remaining mice were closely monitored for autoimmune disease development and survival. The most notable effect of GILZ mRNA nanoparticle treatment on disease pathogenesis was a dramatic increase in life span. GILZ-treated MRL-lpr mice survived to 47 weeks of age, which is a highly significant extension of life span when compared to control mice treated with GFP mRNA nanoparticles (median survival = 25 weeks), all of which had to be euthanized because of advanced disease by that time (Fig. 3b). To elucidate the extended survival, we first evaluated the effects of GILZ expression on serum levels of anti-dsDNA autoantibodies, which are linked to glomerulonephritis in lupus [29]. Six weeks after the treatment start, treatment with GILZ mRNA nanoparticles had reduced the titer of anti-dsDNA antibodies by 3.1-fold compared to the no-treatment controls (Fig. 3c). Histopathology of kidney sections confirmed that GILZ programming had reduced the amount of cellular infiltrate in glomeruli and largely prevented IgG deposits (Fig. 3d-f). In MRL-lpr mice, autoimmune disease also manifests as a skin disorder that begins with alopecia and progresses to skin

lesions and scarring [27]. To examine the skin pathology in treated and control mice, we compared hematoxylin and eosin (H&E)-stained skin sections by microscopy (Fig. 3g). At 20 weeks, when the control mice had cell infiltrates and inflammation progressing to acanthosis and hyperkeratosis, the GILZ mRNA nanoparticle-treated MRL-lpr mice had nearly normal skin architecture. The notable differences in pathology scores between GILZ nanoparticle-treated and control MRL-lpr mice (Fig. 3h) confirmed that GILZ therapy alleviates diverse lupus manifestations. Furthermore, lymph node weights were significantly decreased, by an average 2.1-fold ($P = 0.0015$), after GILZ nanoparticle treatment compared to controls (Fig. 3i). A more detailed breakdown of different B-cell subsets by flow cytometry revealed that, in particular, marginal zone B cells ($CD19^{+}CD23^{-}CD21^{high}$) and plasmablasts ($CD19^{int}$, $B220^{int}$, $CD138^{hi}$, $TACI^{hi}$) were present at lower frequencies in lymph nodes isolated from GILZ nanoparticle-treated animals (3.1-fold and 4.6-fold reduced, respectively, $P < 0.0001$; Fig. 3j, k). This is an important observation because B-cell hyperactivity with increased plasma cell differentiation and enlarged marginal zones are disease hallmarks of lupus in MRL-lpr mice [27]. We could also measure the effects of GILZ-nanoparticle treatment in splenocytes, where we found an average 6.3-fold fewer activated CD4 T cells, as assessed by CD44 and CD69 (Fig. 3l, m).

3.3. Understanding the mechanism of action of GILZ mRNA nanoparticles

To determine the mechanism underlying the therapeutic effects of GILZ mRNA nanoparticles, we first tested whether GILZ overexpression in macrophages interferes with nuclear factor κB (NF-κB) as one of the key pro-inflammatory mediators of autoimmune diseases [30]. To this end, we analyzed NF-κB pathway activation in THP-1 NF-κB luciferase reporter monocytes, following transfection with increasing concentrations of nanoparticles loaded with GILZ-mRNA or control GFP-mRNA (Fig. 4a). We found that overexpressing GILZ in monocytes at the highest mRNA dose tested (1.5 μg/10^6 cells) caused a 3.1-fold reduction in NF-κB activity (Fig. 4b), which is in line with previous reports describing GILZ-induced inhibition of NF-κB [31]. To gain a better understanding of how GILZ-mRNA transfection affects macrophage functions and dynamics, we used *in vivo* bioluminescent imaging. The activatable XenoLight RediJect Inflammation Probe (PerkinElmer) is a silent probe that becomes chemiluminescent following its activation by means of the myeloperoxidase (MPO) activity of phagocytes that are present at the inflammation site. Lupus MRL-lpr mice were serially monitored with XenoLight RediJect following GILZ mRNA nanoparticle treatment, GFP mRNA control nanoparticle treatment or no therapy (Fig. 4c). With progression of lupus, untreated mice showed a gradual increase in bioluminescent signal, in particular in areas overlaying lymphoid tissue. GILZ-encoding, but not GFP-encoding, nanoparticles reduced MPO activity in phagocytes by 9.1-fold ($P < 0.0001$; Fig. 4d), again underlining the broad anti-inflammatory activity of GILZ. To understand in more detail how GILZ overexpression affects signature gene expression in macrophages in SLE, we performed a NanoString gene expression analysis on CD11b + cells isolated from the peripheral blood of nanoparticle-treated vs. untreated mice (Fig. 4e). We found downregulation of a wide range of key genes that directly mediate inflammation or allow homing of monocytes to inflamed tissues, as a result of GILZ therapy (Fig. 4f). Reducing CXC chemokine ligand 16 (Cxcl16) expression on monocytes (Fig. 4g), for instance, is known to attenuate inflammation by disabling invasion of monocytes/

macrophages [32]. Also, blockage of vascular endothelial growth factor C (Vegfc, reduced by 1.8-fold) has been shown to alleviate chronic inflammation by preventing migration of disease-causing lymphocytes in variety of disease models [33]. The calcium-binding protein S100A4, which was downregulated 1.7-fold, has been described to promote pathological inflammation in experimental autoimmune and inflammatory disorders [34,35]. Similarly, upregulation of cathepsin S (CTSS), a protease located in lysosomes or endosomes of professional antigen-presenting cells (reduced 1.4-fold in our experiment), has been reported to be involved in the pathogenesis of autoimmune disease [36]. We also measured significantly lower expression of Toll-like receptors (Tlr7 and Tlr8), as the more traditional mediators of activation signals in macrophages [37], as well as decreased expression of the costimulatory molecule CD86, which is essential to induce T-cell activation [38]. These data establish that nanoparticle-mediated expression of GILZ has a broad spectrum of action to skew inflammatory monocytes/macrophages toward a more neutral phenotype.

4. Discussion

Chronic autoimmune diseases, such as SLE, are challenging to manage owing to their clinical heterogeneity and often unknown causes. Therapies now used in the clinic are corticosteroids, antimalarial drugs, or other systemically acting immunosuppressants. Since these standard therapeutics do not prevent disease progression in most patients, more aggressive drugs such as rituximab (Rituxan) or cyclophosphamide are sometimes prescribed off-label [39,40]. More targeted therapies for autoimmune diseases do exist. For instance, the monoclonal antibody belimumab (Benlysta), which targets B-lymphocyte stimulator (BLyS) on autoreactive B cells in SLE patients, was approved by the US Food and Drug Administration [41]. Nonetheless, in phase III trials, this drug was not vastly superior to placebo and had no therapeutic benefit in African-American patients, which highlights the need to develop novel treatment strategies [42]. Injectable agents that genetically modify immune cells directly within the body to improve their therapeutic action are coming to the fore in translational research and are poised to change the way we treat disease [43]. The driving forces behind this development were fundamental advances in the technology of gene transfer (*i.e.*, vehicles to transport genes into target cells) but also the emergence of synthetic mRNA as a new drug class [44].

In this study, we explored the use of IVT mRNA to rationally reprogram myeloid cells as a strategy to treat autoimmune disease. Our decision to transiently overexpress GILZ was primarily guided by reports describing the important regulatory role of GILZ in SLE [22]. Our group also tested expressing a panel of interferon regulatory factors (IRFs) with known immunosuppressive functions, such as IRF4 or IRF8, but did not achieve relevant anti-inflammatory effects using our platform. Targeting nanoparticles to the Fc γ receptor I (CD64) was an attractive choice, given that CD64-targeting therapeutics, such as immunotoxins, have already entered the clinic [20]. This clinical experience with CD64-directed immunotherapy and the availability of clinical-grade high-affinity antibodies will likely facilitate translation of GILZ-mRNA nanoparticles into human studies.

Patient compliance with repeat nanoparticle dosing and costs are obvious factors that need to be considered when developing this platform into a therapy. The price of

targeted mRNA nanomedicine could compete with frontline *therapeutic* options such as small molecule drugs or monoclonal antibodies, as synthetic mRNA nanodrugs can be produced in bulk quantities just like conventional pharmaceuticals. Several continuous flow microfluidics platforms designed for scalable manufacturing of nanoparticles under GMP conditions are now available [45,46]. These instruments enable scale-independent synthesis of nanoparticles that can be increased from milligram to gram amounts in a single day [47]. This means that nanomedicines could be readily fabricated in a stable form on a large scale, would be easy to distribute as lyophilized reagents, would be inexpensive to administer, and could be delivered to sizeable patient populations in outpatient settings. As for patient compliance, the key advantages for patients receiving mRNA-based nanodrugs are, in our opinion: (**1**) Safety. Uncontrolled insertional mutations are avoided because the delivered mRNA exerts its function in the cytoplasm. (**2**) Speed. In contrast to DNA nanocarriers, synthetic mRNA molecules are directly translated into therapeutic target proteins without the need to enter the nucleus, ensuring high transfection rates and rapid therapeutic effects. (**3**) High transgene copy number per nanoparticle owing to the trim size of the mRNA molecules (no promoter required), and (**4**) Predictable pharmacokinetic profile and therapeutic effects just as for a conventional drug. This would give physicians control over the therapeutic response but also allow them to quickly discontinue therapy should toxicities arise.

Our next step toward clinical translation is to extend our collaboration with the Nanoparticle Characterization Laboratory (NCL) to identify potential infusion reaction risks, with reference to FDA regulations for nanomedicine. Infusion reactions are complex, immune-mediated side effects that mainly occur within minutes to hours of receiving a therapeutic dose of intravenously administered pharmaceutical products [48]. Although infusion reactions are not unique to nanomedicines, they represent a hurdle for the translation of nanotechnology-based drug products, and would be unacceptable in the setting of treating SLE patients. These reactions can range in severity from minor skin rash to anaphylactoid shock and death [49]. Identifying the risk of infusion reactions early in the drug development process can help mitigate potential safety concerns once the product reaches clinical trials, saving developers both time and money—and saving patients from potentially dangerous complications.

5. Conclusions

Taken together, our study provides proof-of-concept that nanotherapeutics based on GILZ-encoding mRNA are worth pursuing as drug candidates for SLE patients. Given the growing body of evidence suggesting that inflammatory myeloid cells play key roles in the pathogenesis of other conditions, such as rheumatoid arthritis [50], ulcerative colitis [51], multiple sclerosis [52], Sjögren's syndrome [53], and even graft-*versus*-host disease [54], this approach could be explored as a therapeutic for a range of diseases.

Supplementary Material

Refer to Web version on PubMed Central for supplementary material.

Acknowledgments

We thank the *FHCRC Genomics Core* staff for assistance in the preparation and analysis of the NanoString gene expression assays.

Funding

This work was supported in part by the *FHCRC Immunotherapy Initiative* with funds provided by the Bezos Family Foundation, by the Comparative Medicine Shared Resource of the Fred Hutchinson/University of Washington Cancer Consortium (P30 CA015704), and the NCI (CA207407). M. Stephan was also supported by a 2018 Emerging Leader Award from the Mark Foundation for Cancer Research, a 2018 Investigator Award from the Alliance for Cancer Gene Therapy (ACGT), and an Allen Distinguished Investigator Award from the Paul G. Allen Frontiers Group.

References

[1]. Amodio G, et al. , Role of myeloid regulatory cells (MRCs) in maintaining tissue homeostasis and promoting tolerance in autoimmunity, inflammatory disease and transplantation, Cancer Immunol. Immunother 68 (2019) 661–672. [PubMed: 30357490]

[2]. Ma WT, Gao F, Gu K, Chen DK, The role of monocytes and macrophages in autoimmune diseases: a comprehensive review, Front. Immunol 10 (2019) 1140. [PubMed: 31178867]

[3]. Barnie PA, et al. Myeloid-derived suppressor cells and myeloid regulatory cells in cancer and autoimmune disorders, Exp. Ther. Med 13 (2017) 378–388. [PubMed: 28352304]

[4]. Pawelec G, Verschoor CP, Ostrand-Rosenberg S, Myeloid-derived suppressor cells: not only in tumor immunity, Front. Immunol 10 (2019) 1099. [PubMed: 31156644]

[5]. Li P, Zheng Y, Chen X, Drugs for autoimmune inflammatory diseases: from small molecule compounds to anti-TNF biologies, Front. Pharmacol 8 (2017) 460. [PubMed: 28785220]

[6]. Stojan G, Petri M, The risk benefit ratio of glucocorticoids in SLE: have things changed over the past 40 years? Curr. Treatm. Opt. Rheumatol 3 (2017) 164–172. [PubMed: 28840094]

[7]. D'Haens GR, van Deventer S, 25 years of anti-TNF treatment for inflammatory bowel disease: lessons from the past and a look to the future, Gut 70 (7) (2021) 1396–1405, 10.1136/gutjnl-2019-320022. Epub 2021 Jan 11. [PubMed: 33431575]

[8]. Lorenzo-Vizcaya A, Isenberg DA, The use of anti-TNF-alpha therapies for patients with systemic lupus erythematosus. Where are we now? Expert. Opin. Biol. Ther (2021) 1–9.

[9]. Roda G, Jharap B, Neeraj N, Colombel JF, Loss of response to anti-TNFs: definition, epidemiology, and management, Clin. Transl. Gastroenterol 7 (2016), e135. [PubMed: 26741065]

[10]. Guerra I, et al. , Induction of psoriasis with anti-TNF agents in patients with inflammatory bowel disease: a report of 21 cases, J. Crohns Colitis 6 (2012) 518–523. [PubMed: 22398059]

[11]. Rosborough BR, Raich-Regue D, Turnquist HR, Thomson AW, Regulatory myeloid cells in transplantation, Transplantation 97 (2014) 367–379. [PubMed: 24092382]

[12]. Lee JH, et al. , Tolerogenic dendritic cells are efficiently generated using minocycline and dexamethasone, Sci. Rep 7 (2017) 15087. [PubMed: 29118423]

[13]. Poltavets AS, Vishnyakova PA, Elchaninov AV, Sukhikh GT, Fatkhudinov TK, Macrophage modification strategies for efficient cell therapy, Cells 9 (2020).

[14]. Van Hoecke L, Roose K, How mRNA therapeutics are entering the monoclonal antibody field, J. Transl. Med 17 (2019) 54. [PubMed: 30795778]

[15]. Cross R, Can mRNA disrupt the drug industry? Chem. Eng. News 96 (2018) 34–40.

[16]. Kariko K, et al. , Incorporation of Pseudouridine into mRNA yields superior nonimmunogenic vector with increased translational capacity and biological stability, Mol. Ther 16 (2008) 1833–1840. [PubMed: 18797453]

[17]. Nallagatla SR, Bevilacqua PC, Nucleoside modifications modulate activation of the protein kinase PKR in an RNA structure-specific manner, Rna 14 (2008) 1201–1213. [PubMed: 18426922]

[18]. Kariko K, Weissman D, Naturally occurring nucleoside modifications suppress the immunostimulatory activity of RNA: implication for therapeutic RNA development, Curr. Opin. Drug Disc 10 (2007) 523–532.

[19]. Muttach F, Muthmann N, Rentmeister A, Synthetic mRNA capping, Beilstein J. Org. Chem 13 (2017) 2819–2832. [PubMed: 30018667]

[20]. Akinrinmade OA, et al. , CD64: an attractive immunotherapeutic target for M1-type macrophage mediated chronic inflammatory diseases, Biomedicines 5 (2017).

[21]. D'Adamio F, et al. , A new dexamethasone-induced gene of the leucine zipper family protects T lymphocytes from TCR/CD3-activated cell death, Immunity 7 (1997) 803–812. [PubMed: 9430225]

[22]. Bereshchenko O, Migliorati G, Bruscoli S, Riccardi C, Glucocorticoid-induced Leucine zipper: a novel anti-inflammatory molecule, Front. Pharmacol 10 (2019) 308. [PubMed: 30971930]

[23]. Mohammadi S, Ebadpour MR, Sedighi S, Saeedi M, Memarian A, Glucocorticoid-induced leucine zipper expression is associated with response to treatment and immunoregulation in systemic lupus erythematosus, Clin. Rheumatol 36 (2017) 1765–1772. [PubMed: 28601944]

[24]. Ronchetti S, Gentili M, Ricci E, Migliorati G, Riccardi C, Glucocorticoid-induced Leucine zipper as a Druggable target in inflammatory bowel diseases, Inflamm. Bowel Dis 26 (2020) 1017–1025. [PubMed: 31961437]

[25]. Yang N, Baban B, Isales CM, Shi XM, Role of glucocorticoid-induced leucine zipper (GILZ) in inflammatory bone loss, PLoS One 12 (2017), e0181133. [PubMed: 28771604]

[26]. Sevilla LM, Perez P, Glucocorticoids and glucocorticoid-induced-Leucine-zipper (GILZ) in psoriasis, Front. Immunol 10 (2019) 2220. [PubMed: 31572404]

[27]. Killian M, Batteux F, Paul S, The MRL/lpr mouse model: an important animal model for systemic Sjogren syndrome and Polyautoimmunity, J. Rheumatol 47 (2020) 157. [PubMed: 31523043]

[28]. Parayath NN, Stephan SB, Koehne AL, Nelson PS, Stephan MT, In vitro-transcribed antigen receptor mRNA nanocarriers for transient expression in circulating T cells in vivo, Nat. Commun 11 (2020) 6080. [PubMed: 33247092]

[29]. Yung S, Chan TM, Mechanisms of kidney injury in lupus nephritis - the role of anti-dsDNA antibodies, Front. Immunol 6 (2015) 475. [PubMed: 26441980]

[30]. Miraghazadeh B, Cook MC, Nuclear factor-kappaB in autoimmunity: man and mouse, Front. Immunol 9 (2018) 613. [PubMed: 29686669]

[31]. Di Marco B, et al. , Glucocorticoid-induced leucine zipper (GILZ)/NF-kappaB interaction: role of GILZ homo-dimerization and C-terminal domain, Nucleic Acids Res. 35 (2007) 517–528. [PubMed: 17169985]

[32]. Garcia GE, et al. , Inhibition of CXCL16 attenuates inflammatory and progressive phases of anti-glomerular basement membrane antibody-associated glomerulonephritis, Am. J. Pathol 170 (2007) 1485–1496. [PubMed: 17456756]

[33]. Carvalho JF, Blank M, Shoenfeld Y, Vascular endothelial growth factor (VEGF) in autoimmune diseases, J. Clin. Immunol 27 (2007) 246–256. [PubMed: 17340192]

[34]. Sumova B, et al. , Circulating S100 proteins effectively discriminate SLE patients from healthy controls: a cross-sectional study, Rheumatol. Int 39 (2019) 469–478. [PubMed: 30392117]

[35]. Turnier JL, et al. , Urine S100 proteins as potential biomarkers of lupus nephritis activity, Arthritis Res. Ther 19 (2017) 242. [PubMed: 29065913]

[36]. Kim SJ, et al. , Increased cathepsin S in Prdm1(−/−) dendritic cells alters the TFH cell repertoire and contributes to lupus, Nat. Immunol 18 (2017) 1016–1024. [PubMed: 28692065]

[37]. Wu YW, Tang W, Zuo JP, Toll-like receptors: potential targets for lupus treatment, Acta Pharmacol. Sin 36 (2015) 1395–1407. [PubMed: 26592511]

[38]. Herrada AA, et al. , Innate immune Cells' contribution to systemic lupus Erythematosus, Front. Immunol 10 (2019) 772. [PubMed: 31037070]

[39]. Ryden-Aulin M, et al. , Off-label use of rituximab for systemic lupus erythematosus in Europe, Lupus Sci. Med 3 (2016), e000163. [PubMed: 27651920]

[40]. Sigdel MR, Kafle MP, Shah DS, Outcome of low dose cyclophosphamide for induction phase treatment of lupus nephritis, a single center study, BMC Nephrol. 17 (2016) 145. [PubMed: 27717323]

[41]. Srivastava A, Belimumab in systemic lupus Erythematosus, Indian J. Dermatol 61 (2016) 550–553. [PubMed: 27688447]

[42]. Mahieu MA, Strand V, Simon LS, Lipsky PE, Ramsey-Goldman R, A critical review of clinical trials in systemic lupus erythematosus, Lupus 25 (2016) 1122–1140. [PubMed: 27497257]

[43]. Parayath NN, Stephan MT, In situ programming of CAR T cells, Annu. Rev. Biomed. Eng 23 (2021) 385–405, 10.1146/annurev-bioeng-070620-033348. April 16, 2021. [PubMed: 33863239]

[44]. Sahin U, Kariko K, Tureci O, mRNA-based therapeutics–developing a new class of drugs, Nat. Rev. Drug Discov 13 (2014) 759–780. [PubMed: 25233993]

[45]. Operti MC, et al. , A comparative assessment of continuous production techniques to generate sub-micron size PLGA particles, Int. J. Pharm 550 (2018) 140–148. [PubMed: 30144511]

[46]. Leaver T Nanoparticles - a revolution in the development of drug delivery vehicles. Drug Dev. Deliv

[47]. Petschacher C, E.A, Besenhard M, Wagner J, Barthelmes J, Bernkop-Schnuerch A, Khinast JG, Zimmer A, Thinking continuously: a microreactor for the production and scale-up of biodegradable, self-assembled nanoparticles, Polym. Chem 4 (2013) 2342–2352.

[48]. Handbook of Immunological Properties of Engineered Nanomaterials, Front Nanobiomed. Res 1 (2013) 1–692.

[49]. Mocan T, et al. , Hypersensitivity and nanoparticles: update and research trends, Clujul Med. 89 (2016) 216–219. [PubMed: 27152071]

[50]. Siouti E, Andreakos E, The many facets of macrophages in rheumatoid arthritis, Biochem. Pharmacol 165 (2019) 152–169. [PubMed: 30910693]

[51]. Jones GR, et al. , Dynamics of colon monocyte and macrophage activation during colitis, Front. Immunol 9 (2018) 2764. [PubMed: 30542349]

[52]. Chu F, et al. , The roles of macrophages and microglia in multiple sclerosis and experimental autoimmune encephalomyelitis, J. Neuroimmunol 318 (2018) 1–7. [PubMed: 29606295]

[53]. Ushio A, et al. , CCL22-producing resident macrophages enhance T cell response in Sjogren's syndrome, Front. Immunol 9 (2018) 2594. [PubMed: 30467506]

[54]. Alexander KA, et al. , CSF-1-dependant donor-derived macrophages mediate chronic graft-versus-host disease, J. Clin. Invest 124 (2014) 4266–4280. [PubMed: 25157821]

[55]. Kuriakose J, et al. , Patrolling monocytes promote the pathogenesis of early lupus-like glomerulonephritis, J. Clin. Invest 129 (2019) 2251–2265. [PubMed: 31033479]

[56]. Chan OT, et al. , Deficiency in beta(2)-microglobulin, but not CD1, accelerates spontaneous lupus skin disease while inhibiting nephritis in MRL-Fas(lpr) nice: an example of disease regulation at the organ level, J. Immunol 167 (2001) 2985–2990. [PubMed: 11509649]

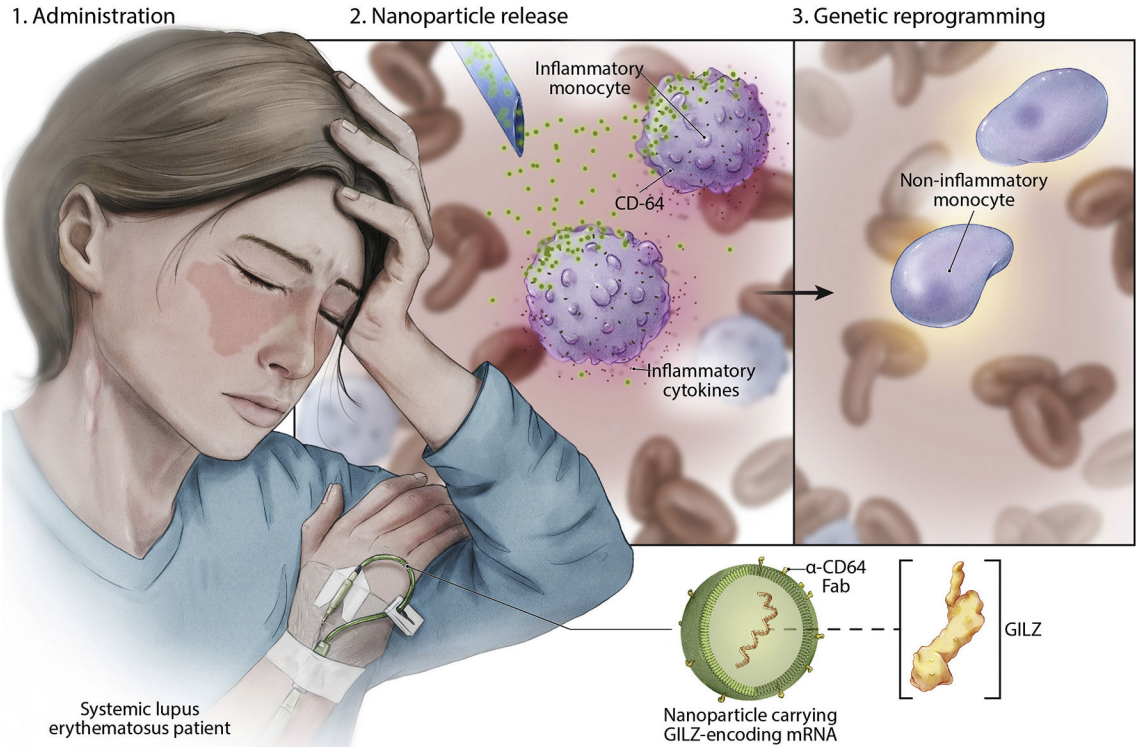

Fig. 1.

Schematic illustrating how we reprogram circulating inflammatory myeloid cells with potent immunosuppressive functions using targeted mRNA nanoparticles. These particles are coated with anti-CD64 ligands, so once they are infused into the patient's circulation (exemplified in a systemic lupus erythematosus patient), they can transfer the transgenes they carry into inflammatory monocytes to imprint an immunosuppressive phenotype. Illustrated is a nanoparticle carrying mRNA encoding a master regulator of anti-inflammatory responses, glucocorticoid-induced leucine zipper (*GILZ*).

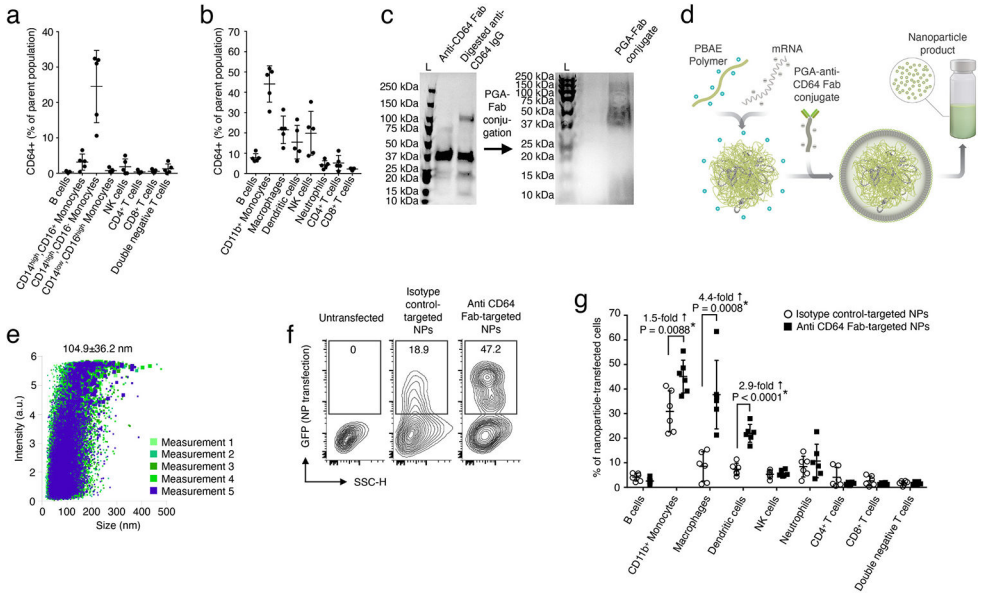

Fig. 2.

Designing nanoparticles to choreograph IVT mRNA transfection of inflammatory myeloid cells. Flow-cytometry analysis of CD64 expression on various immune cells in whole blood from patients with systemic lupus erythematosus (SLE) (a) or MRL/lpr lupus mice at 10 weeks of age (b). (c) SDS gel electrophoresis showing the anti-CD64 Fab fragment after limited digestion of anti-CD64 IgG by papain (left panel), and following coupling to polyglutamic acid (PGA; right panel). (d) Diagram describing how we fabricated the nanoparticles. (e) Size distributions, measured using a NanoSight NS300 instrument. The mean diameter ± SD is indicated at the top. $N = 5$ independently manufactured nanoparticle batches. (f) Gene transfer efficiencies into CD64-expressing RAW264.7 mouse macrophage cells (pretreated with lipopolysaccharide (LPS) and interferon-gamma to induce an inflammatory CD64+ phenotype) measured by flow cytometry 24 h after transfection with GFP-mRNA nanoparticles. (g) Flow cytometric quantitation of *in vivo* transfection rates in different immune cell subpopulations of 10-week-old MRL/lpr lupus mice 48 h after a single intravenous dose of isotype control-targeted *versus* anti-CD64 Fab-targeted nanoparticles carrying GFP mRNA.

B cells (CD45+, CD3−, CD19+), Monocytes (CD45+, CD3−, LY6G−, CD11b+), Macrophages (CD45+, CD3−, LY6G−, CD11b+, F4/80+), Dendritic cells (CD45+, CD3−, LY6G−, CD11b+, F4/80−, CD11c+), NK cells (CD45+, CD3−, NK1.1+), Neutrophils (CD45+, CD3−, Ly6G+), and T cells [CD4+ T cells (CD45+, CD3+, CD4+, CD8−), CD8+ T cells (CD45+, CD3+, CD4−, CD8+).

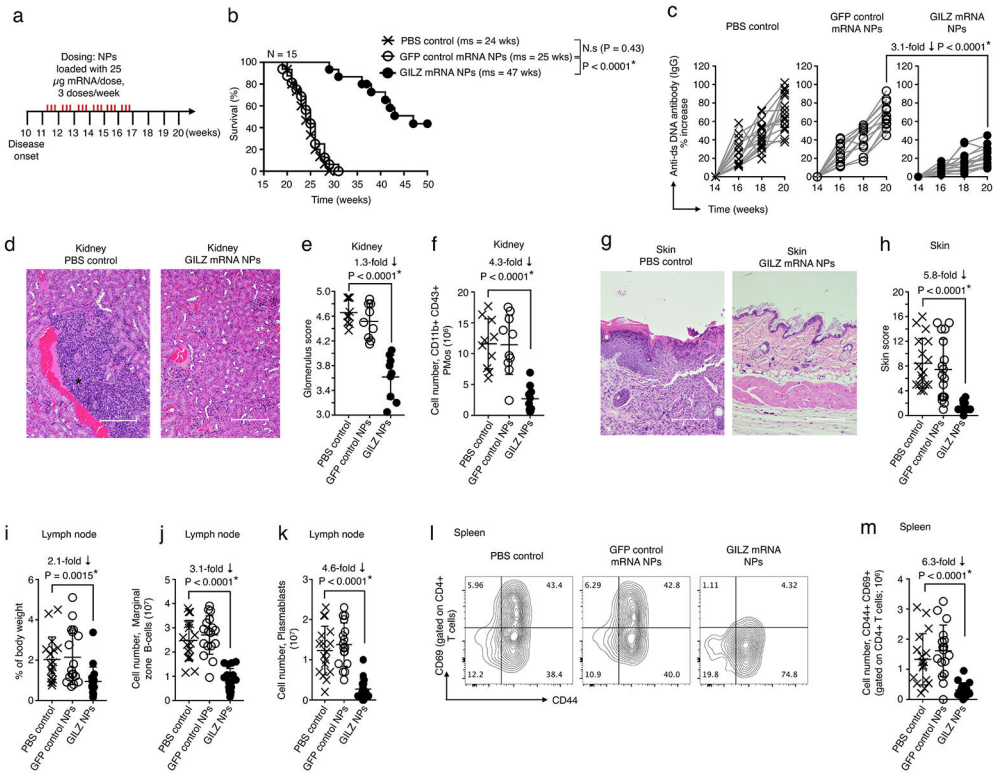

Fig. 3.

Suppression of lupus nephritis and skin lesions in MRL/lpr mice by administration of GILZ-encoding nanoparticles. (a) Time line and nanoparticle (NP) dosing regimen. (b) Survival of animals following therapy, depicted as Kaplan–Meier curves. Shown are 15 mice per treatment group pooled from three independent experiments. ms, median survival. Statistical analysis between the treated experimental and the untreated control group was performed using the Log-rank test; $P < 0.05$ was considered significant. (c) Comparison of autoantibody (anti-ds-DNA IgG) serum levels. (d) Representative H&E-stained sections of kidneys isolated from PBS controls or GILZ mRNA nanoparticle-treated MRL/lpr lupus mice. Scale bars, 200 <m. (e) Kidney glomerulus scores (using the system described by Kuriakose J et al. [55]). Total numbers of CD11b + CD43+ Patrolling monocytes (PMos) isolated from kidneys are shown in (f). (g) Representative H&E-stained sections of skin isolated from PBS controls or GILZ mRNA nanoparticle-treated MRL/lpr lupus mice. Scale bars, 200 μm. (h) Skin inflammation was scored using the system described by Chan et al. [56] (i) The graph represents total lymph node weights (left and right; Axillary, Brachial and Inguinal lymph nodes). Statistical analysis was performed using one-way ANOVA. Cell numbers of marginal zone B cells ($CD19^{+}CD23^{-}CD21^{high}$) and plasmablasts ($CD19^{int}$, $B220^{int}$, $CD138^{hi}$, $TACI^{hi}$) are shown in (j) and (k), respectively. (l) Multicolor flow cytometry analysis of activated (CD69+) CD4+ splenocytes. Absolute numbers are shown in (m).

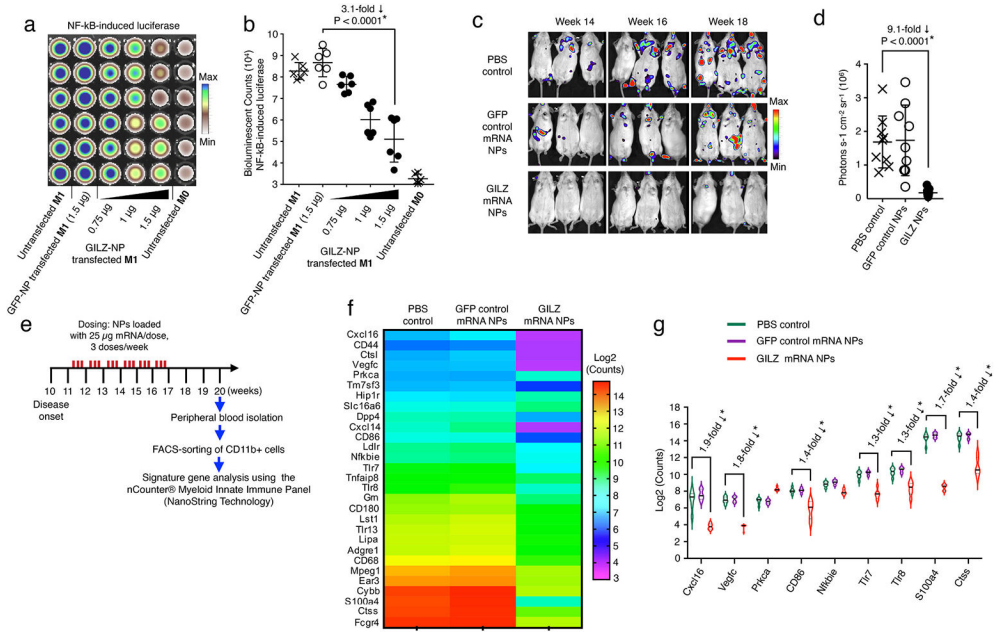

Fig. 4.

Human GILZ mRNA-carrying nanoparticles reprogram human macrophages to perform anti-inflammatory functions by downregulating key signature genes. (a) Bioluminescent imaging of differentiated THP1-Lucia cells (pro-inflammatory) cultured in 96-well plates and transfected with indicated concentrations of nanoparticles carrying human GILZ mRNA *versus* control GFP mRNA. Shown are six representative wells per group. Levels of NF-κB-indueed Lucia luciferase were determined 24 h after transfection using Quanti-Luc. Bioluminescent counts are summarized in the bar graph shown in (b). $N = 6$ biologically independent samples. Shown are mean values ± SD. (c) Serial bioluminescent imaging of myeloperoxidase activity in activated phagocytes post-therapy. Three representative mice from each cohort ($N = 8$) are shown. (d) Quantification of bioluminescent signals at week 18. Each symbol indicates the whole-body bioluminescent photon count per mouse. (e) Experimental time line of the gene expression analysis study. (f) Heat map of anti-inflammatory signature gene expression in monocytes sorted from MRL-lpr SLE mice following therapy. (E) Violin plots showing counts for the indicated genes. N = 6 biologically independent samples.